

# Detecting Space Based Interference on GNSS Signals

Akshata Patil, *Stanford University*, R. Eric Phelts, *Stanford University*, Yu-Hsuan Chen, *Stanford University*, Sherman Lo, *Stanford University*, Todd Walter, *Stanford University*

## Biographies

**Akshata Patil** is a graduate student in the Department of Aeronautics and Astronautics at Stanford University. She graduated with a Bachelor of Science in Aerospace Engineering from Florida Tech in 2020. Her research interests revolve around enhancing the reliability and security of perception and navigation systems used in unmanned aerial vehicles and autonomous driving vehicles.

**R. Eric Phelts** is a research engineer in the Department of Aeronautics and Astronautics at Stanford University. His research involves developing signal monitoring techniques and analysis for SBAS, GBAS, and ARAIM.

**Yu-Hsuan Chen** is a research engineer in the GPS laboratory at Stanford University. He received his Ph.D. in electrical engineering from National Cheng Kung University in 2011.

**Sherman Lo** is a senior research engineer at the Stanford GPS Laboratory and the executive director of the Stanford Center for Position Navigation and Time. He received his Ph.D. in Aeronautics and Astronautics from Stanford University in 2002. He has and continues to work on navigation robustness and safety, often supporting the FAA. He has conducted research on Loran, alternative navigation, SBAS, ARAIM, GNSS for railways and automobiles. He also works on spoof and interference mitigation for navigation. He has published over 100 research papers and articles. He was awarded the ION Early Achievement Award.

**Todd Walter** is a Professor of Research and director of the GPS laboratory at Stanford University.

## ABSTRACT

GNSS receivers operate by relying on satellite signals coming from the Medium Earth Orbit (MEO), but these signals can easily be drowned out by background noise, underscoring the critical importance of interference detection. While traditional methods leaned on local spatial and temporal characteristics for this purpose, the advent of advanced widespread, multi-band GNSS receiver networks have significantly enhanced the capabilities of interference detection.

This paper aims to investigate instances of interference by leveraging the Trimble reference network which consists of 43 multi-frequency receivers deployed all over the US and Europe. In June of 2021, this network detected an unusual power spike within the B3/E6 band at 1268.52 MHz. Further monitoring and analysis unveiled a distinct interference pattern that eliminated the possibility of local jamming and instead pointed to a space-based origin. This conclusion was substantiated by the simultaneous impact on receivers across the entirety of Europe and the U.S. over a mere 24-hour span.

This paper draws upon data collected from GNSS receivers scattered across these two continents to undertake interference monitoring. By analyzing averaged FFT (Fast Fourier Transforms) data in the B3/E6 band, the study correlates this information with LOS observables obtained from each receiver. Ultimately, the paper endeavors to determine the interference's global trajectory and pinpoint the most probable space-based origin. In addition, it attempts to assess any effects on a receiver position solution. Such monitoring is of paramount importance in safeguarding the quality and reliability of GNSS signals.

## 1 INTRODUCTION

Uninterrupted operation of GNSS cannot be guaranteed due to its signals' susceptibility to various forms of disruptions. As, all the GNSS systems rely on the ability to receive a weak signal from over 20,000 km away in space, making it inherently fragile to Radio Frequency Interference (RFI). The impact of interference in GNSS data cannot be emphasized enough. GNSS signal disruptions

hinder the progress of GNSS-based technology and services. As a result, there has been a constant battle to continue to protect, toughen and augment these signals to ensure integrity for its users.

In response to the growing demand for reliable and accurate GNSS data, Trimble Inc, a prominent commercial GNSS equipment and service provider, has deployed a network consisting of 43 multi-frequency receivers spanning both the United States and Europe. Each of these receivers possesses the capability to generate Fast Fourier Transforms (FFT) data for multiple frequency bands. In each band, the spectrum data is averaged for one minute. This functionality enables users to analyze the mean and standard deviation of signal power across various frequency bands.

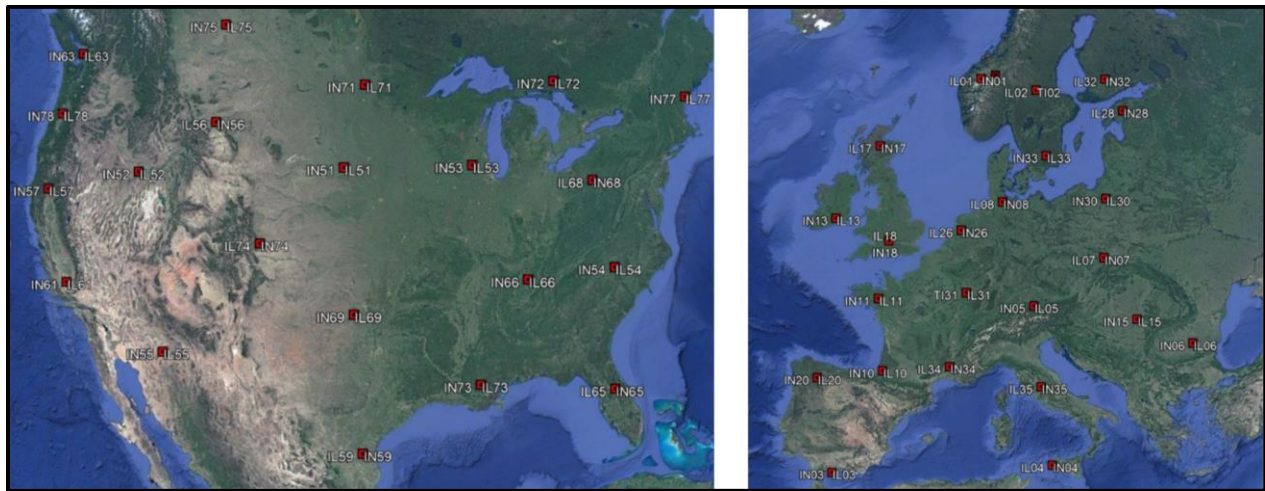


**FIGURE 1:** Trimble's Receiver Network

In June of 2021, utilizing this network of receivers, Trimble detected an unusual spike in signal power within the B3-E6 band, specifically at a frequency of 1268.52 MHz, occurring simultaneously in two widely separated locations--Italy in Europe and South Dakota in the United States. Further examination revealed that this spike in signal power was a consistent observation across every receiver deployed throughout both the United States and Europe.

The primary objective of this paper is to find the origin of this interference and assess its potential impact on receiver positioning.

## 2 RELATED RESEARCH

Historically, people have devised a spectrum of spatial (such as Broumandan et al., (2016)) and temporal techniques (Wang, P et al., (2018)) to investigate and address interference, which has been an issue of longstanding concern. Typically, these methodologies involve one or more of the following areas of research per (Ferrara, N. G. et al., 2018):

- **Detection:** The initial step involves recognizing when there is an issue with the received signal. This involves the ability to identify anomalies or irregularities in the signal, indicating the presence of interference (Murrian et al., (2019))
- **Characterization:** Once interference is detected, the next phase entails delving deeper into understanding the characteristics of the unwanted signal.
- **Localization:** This step aims to identify the origin or location of the interference, which could be within the immediate vicinity or emanating from a more distant source per Bhatti, J.A., et al., (2012) and Lindstrom, J. Et al., (2017).
- **Impact Analysis:** Understanding the impact of the interference on the application of interest.
- **Mitigation:** This aims to prevent, reduce, or eliminate any adverse impacts of the interference. The range of mitigation strategies is diverse, encompassing both hardware-based and software-based approaches. Mitigation strategies are not discussed in this paper.

### 3 SIGNAL COMPARISON

To uncover the source of the interference, gaining a comprehensive understanding of its nature is critical. The initial detection phase began with a thorough examination of the interference frequency, which stood at 1268.52 MHz and the satellites transmitting on that frequency.

In 2015, the Chinese Beidou Satellite Navigation System (BDS) unveiled its Beidou 3 satellite constellation, with the goal of expanding regional navigation service offerings. The new constellation, known as BDS-3, was designed provide positioning and timing (PNT) services to the globe, in addition to China's existing regional Beidou constellations BDS-2 constellation (primarily designed to cover the Asia-Pacific region) and BDS-1 (designed to serve only China). This strategic shift towards a global navigation system was part of China's broader endeavor to enhance compatibility with established GNSS networks and reinforce their competitiveness in the global navigation industry.

The B3I signal, transmitted by both the BDS-2 and BDS-3 satellite constellations, operates at a nominal frequency of 1268.520 MHz. This signal bears a strong resemblance to the GPS navigational signal at L5 (1176 MHz). Like the L5 GPS signal, the B3I signal employs Binary Phase Shift Keying (BPSK (10)) modulation and can help provide Positioning, Navigation, and Timing (PNT) services for a wide range of civilian applications. The figure below offers a detailed comparison of the B3I signal alongside other GNSS signals at various frequencies.

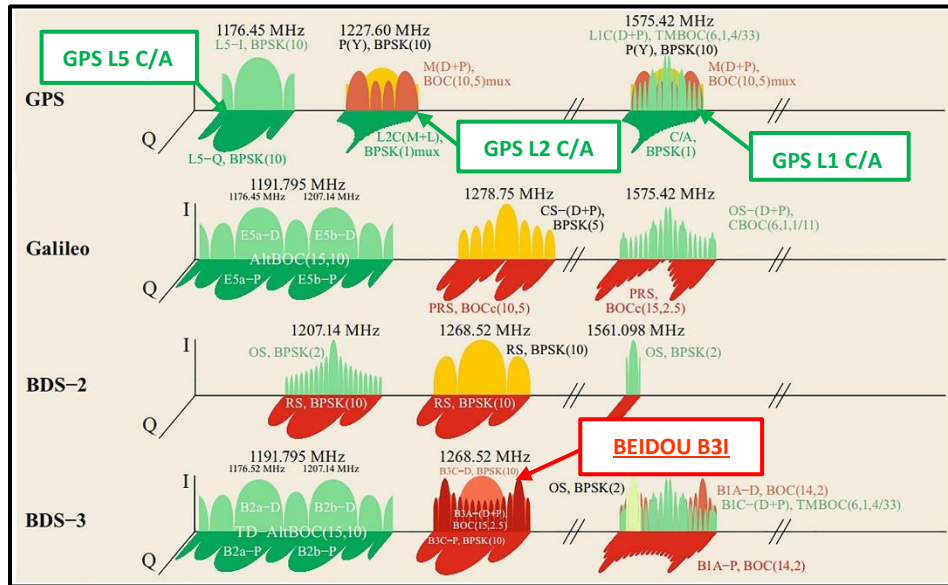


FIGURE 2: Signal Comparison, Courtesy of Theolert S. et al., (2019)

### 4 INVESTIGATION APPROACH

#### 4.1 Detection

Upon conducting an initial investigation of the FFT data, as reported by the network of Trimble receivers, it was evident that the peaks in signal intensity were observed on two separate continents (within a 24-hour period): Europe (Italy, receiver station ID: IN04) and North America (South Dakota, receiver station ID: IN61), specifically on the B3I center frequency. The plot below shows the interference being detected on September 01, 2022. The axes are defined as follows:

- X-axis: Frequency [MHz]. The span of FFT frequencies is centered at 1280 MHz.
- Y-axis: Time [Seconds of GPS Week]
- Z-axis: Mean signal Power measured in decibel [dB].

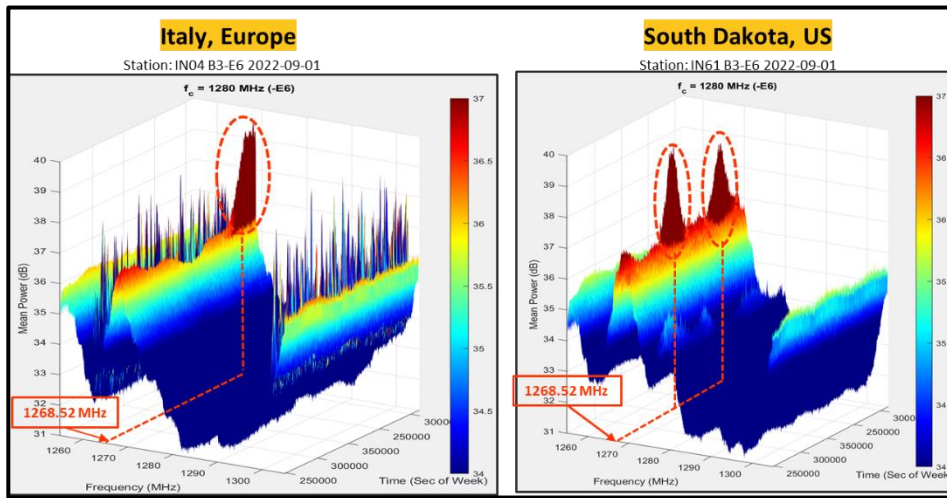


FIGURE 3: Initial Interference Detection

However, upon examining data from additional receiver stations, it became evident that the observed spike in signal intensity wasn't just restricted solely to those two stations. Instead, it exhibited a consistent presence across every receiver station deployed across both Europe and North America during a single 24-hour timeframe. The plot presented below shows a glimpse of the standard deviation recorded at all receiver stations on February 03, 2022. The axes in the plot are defined as follows:

- X-axis: Frequency values [MHz]
- Y-axis: Station ID for each receiver within the Trimble network
- Z-axis: The largest standard deviation recorded at each respective receiver station during a single 24-hour period

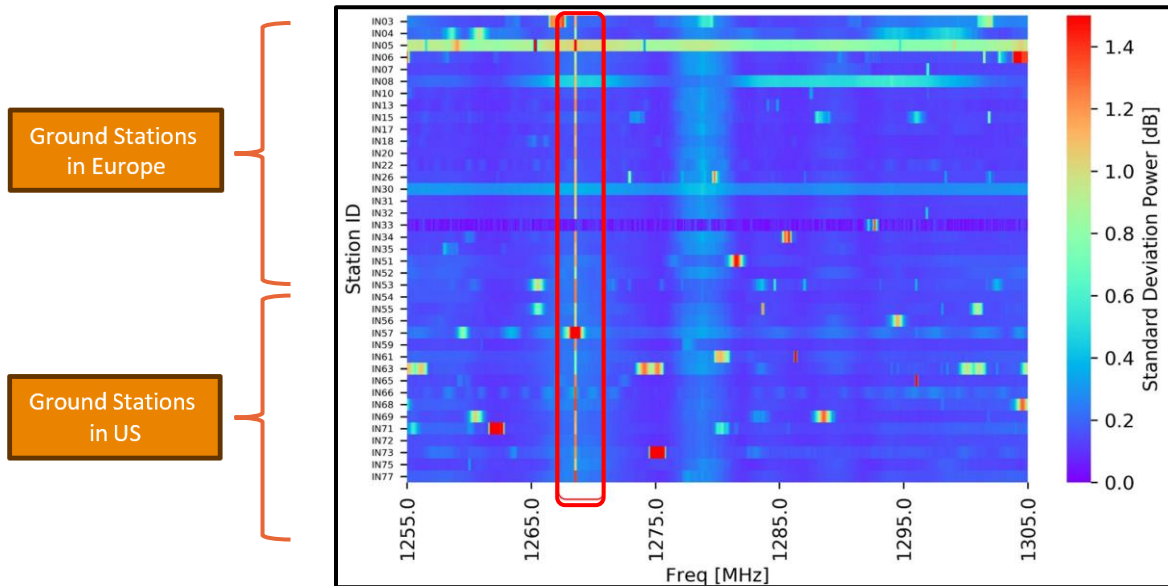


FIGURE 4: B3-E6 Standard Deviation Spectrum for 2022-02-03

The unique interference pattern that extended across two continents quickly ruled out the possibility of the source being a local jamming event and strongly indicated that it could potentially originate from space. And the large number of stations able to view the interference at once indicated it was emanating from Medium Earth Orbit (MEO). Still, because as many as 139 navigational satellites are in MEO, without making additional assumptions about which specific constellation might be the source, it was somewhat challenging to pinpoint the specific satellite responsible for the interference.

## 4.2 Localization

To understand the origin of the interference, it was critical to understand its trajectory. Therefore, a systematic approach towards localization was taken through the following steps:

- 1) Monitor using network receivers.
- 2) Extract the path.
- 3) Find common satellites
- 4) Confirm with direct measurements.

The details of each of these steps are described in the subsections that follow.

### 4.2.1 Network Receiver Monitoring

The first step involved monitoring each ground station that was subjected to interference for a continuous 24-hour period. For instance, on April 28, 2023, Sweden (Receiver station ID: IN02) was chosen as the focal point. In Figures 5 and 6 below present an FFT plot depicting 24-hour receiver data acquired in Sweden along with a surface contour view generated at the B3I frequency:

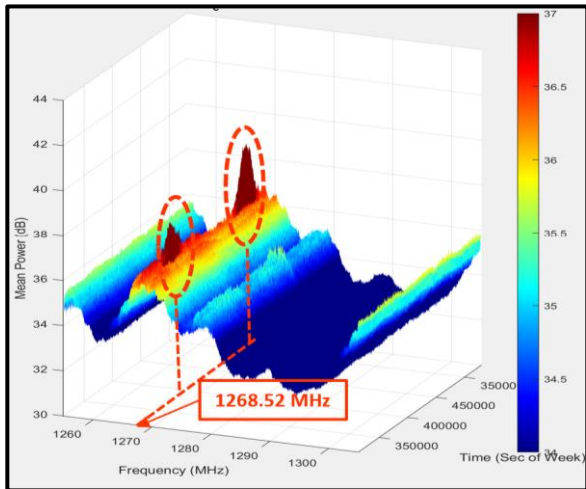


FIGURE 5: FFT Analysis on Receiver IN02 in Sweden

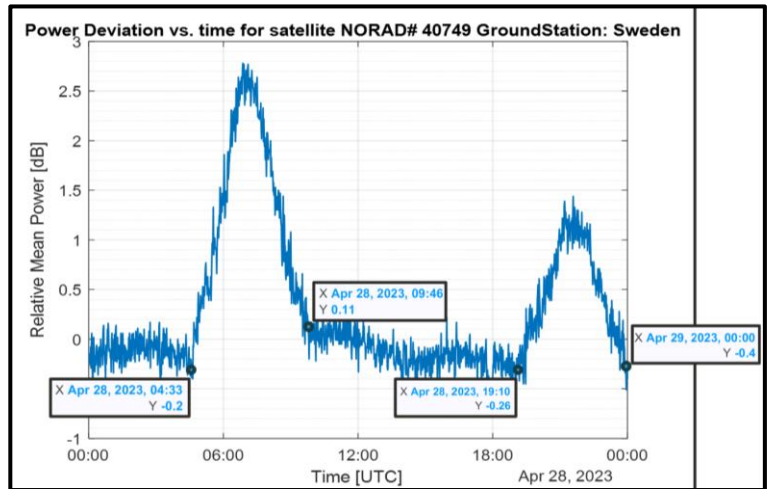


FIGURE 6: FFT Data Contoured at 1268.520 MHz

As evident from the figures above, station IN02 in Sweden experienced two distinct instances of interference on April 28, 2023, both occurring within a single 24-hour period. As observed, each episode of interference endured for approximately 5 hours. Given the narrow focus of interference around the B3I frequency, our initial approach centered on the targeted examination of all the Beidou MEO satellites.

To be clear, the orbital paths of each satellite within the Beidou constellation were tracked. These paths were correlated with precise timestamps of interference occurrences. In essence, whenever the Sweden Trimble station IN02 detected interference, all Beidou satellites were monitored within the receiver's field of view during the interference event. This same procedure was then applied to each receiver spanning both continents to deduce the trajectory of the interference.

To illustrate the effectiveness of this strategy, consider the scenario where receiver A detected interference between 12:00 and 2:00 UTC, and concurrently, receiver B experienced interference from 2:00 to 4:00 UTC. This revealed that the source of interference was moving from receiver A to receiver B. Using this approach, the list of candidate satellites was reduced by monitoring the satellites that were concurrently observed by both receiver A and B.



### 4.2.2 Path Extraction

As of January 2022, the Beidou constellation comprised a total of 44 operational satellites. Among these, 7 are positioned in a geostationary orbit, 10 occupy geosynchronous orbits inclined at  $55^\circ$  (IGSO), while the remaining 27 satellites are situated in the MEO. Out of this set of 27 MEO satellites, our adopted strategy eventually helped to identify a specific satellite within the BDS-3 constellation, identified by NORAD (North American Aerospace Defense Command) ID: 40749.

This satellite's orbital path precisely aligned with the timestamps of interference incidents detected by the receiver station IN02 in Sweden on April 28, 2023. The convergence of these timestamps with the satellite's ground track is illustrated in the plot below. It provides a clear visualization of the instances when the satellite passed directly over the receiver station:

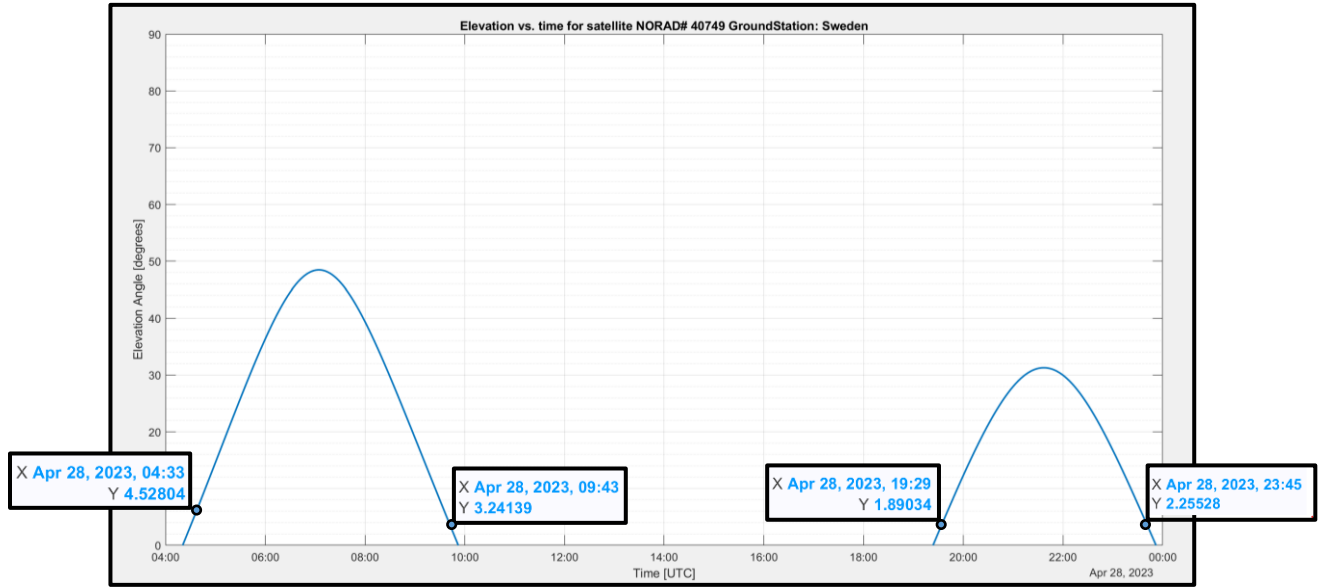


FIGURE 7: Satellite Track over Sweden on April 28, 2023

### 4.2.3 Common Satellite Identification

Although the preceding outcomes unmistakably pointed out the satellite whose trajectory closely aligned with the timestamps of interference, there remained an uncertainty that this alignment at just this one station was coincidental. To rule this out, monitoring was extended to include receiver data from many Trimble stations in Europe and the U.S. on April 28, 2023. The investigation revealed that every Trimble network receiver on both continents exhibited a temporal correlation with the identified satellite, synchronizing with their respective interference timestamps.

The culmination of these findings is shown in Figures 8 to 13. These graphs incorporate a dual-axis format, and these axes are defined as follows:

- X-axis: Time [UTC].
- Y-axis left: Satellite Elevation [ $^\circ$ degrees].
- Z-axis, right: Relative Mean Power [dB]. (This data is centered at the frequency of 1268.520 MHz.)

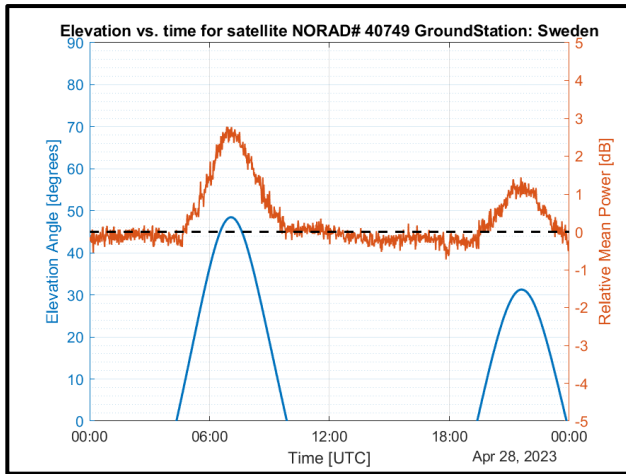


**FIGURE 8:** Interference vs. Satellite Ground Track in Sweden

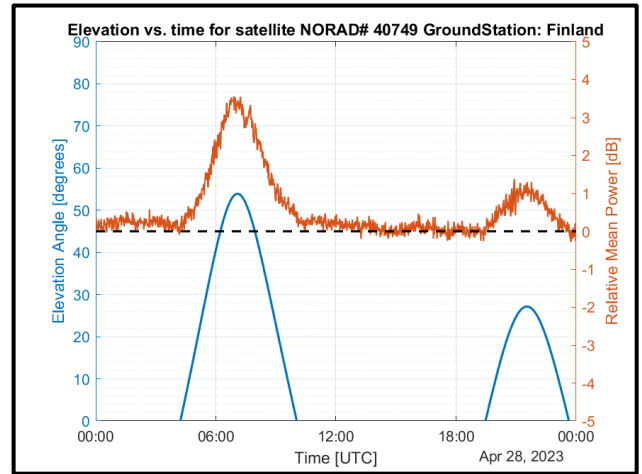


**FIGURE 9:** Interference vs. Satellite Ground Track in Finland

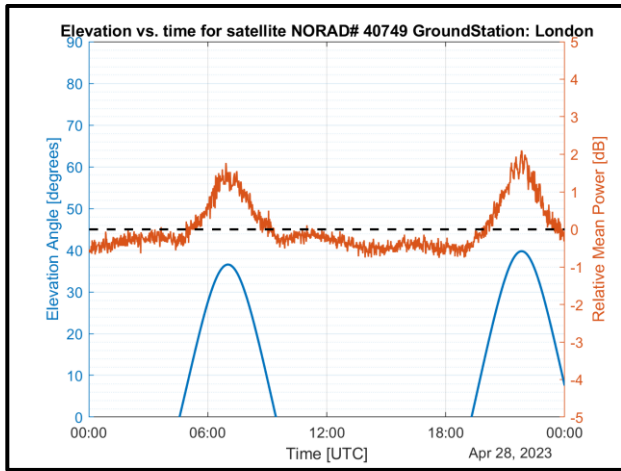


**FIGURE 10:** Interference vs. Satellite Ground Track in London

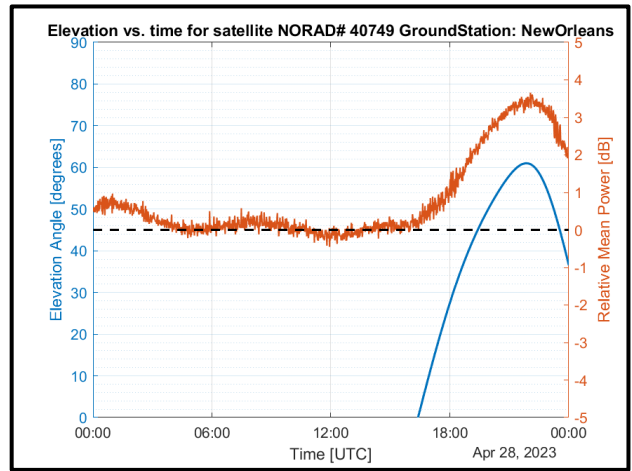


**FIGURE 11:** Interference vs. Satellite Ground Track in New Orleans

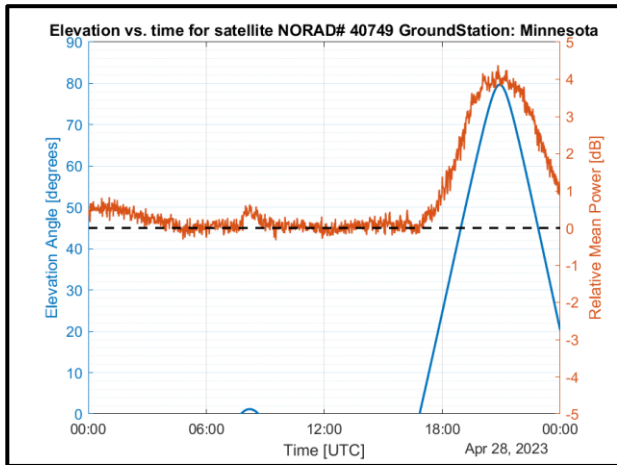


**FIGURE 12:** Interference vs. Satellite Ground Track in Minnesota

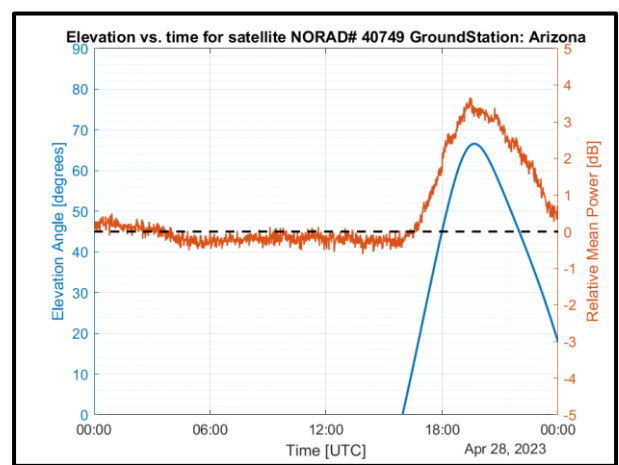


**FIGURE 13:** Interference vs. Satellite Ground Track in Arizona

The above results indicate the interference track travelling from in Sweden, Europe to Arizona, North America on April 28, 2023.

As seen from above plots, the interference can be seen in the signal intensity when 40749 comes into view of stations around the world. Figure 14 below illustrates the ground track of the satellite for April 28, 2023:

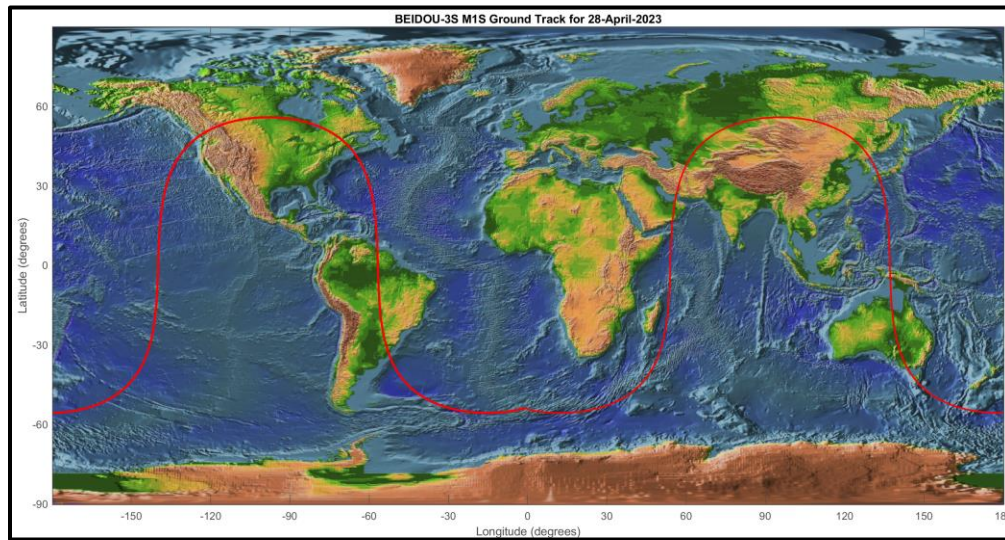


**FIGURE 14:** Satellite 40749 Ground Track

#### 4.2.4 Direct Measurement and Confirmation

To confirm the presence of the interference on the N40749, we conducted a data acquisition test employing a Septentrio Mosaic X5 receiver and a 1.8-meter dish antenna. To measure a nominal B3I signal, the antenna was first pointed towards a randomly selected satellite with NORAD ID: 40376 from the Beidou constellation. As expected the spectrum showed no observable fluctuations in signal strength. Conversely, when the antenna was precisely aligned with satellite 40749, a conspicuous and distinct power spike was readily apparent at the B3I frequency. The results from this test can be observed in Figures 15 and 16 below. Their axes are defined as follows:

- X-axis: Frequency [MHz], The data is centered at the B3I frequency, 1268.520 MHz.
- Y-axis: Signal Power, measured in decibels [dB]

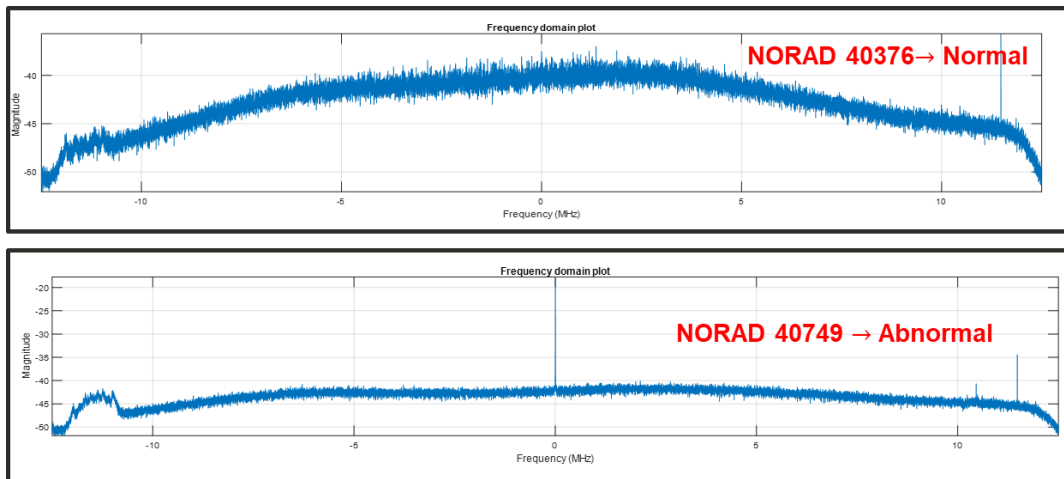


**FIGURE 15 (top):** Data Acquisition Test Performed on Satellite 40376. (Plot centered at 1268.52 MHz)

**FIGURE 16 (bottom):** Data Acquisition Test Performed on Satellite 40749. (Plot centered at 1268.52 MHz)



#### ***4.2.5 Challenges: Incorrect Satellite Labelling***

One of the most unexpected challenges encountered during the localization process was obtaining accurate orbital parameters for the Beidou satellites. Beidou has maintained relatively high confidentiality around its system. This posed a substantial obstacle to accessing the Beidou almanac data, which was necessary for computing precise satellite ground tracks and comprehending their orbital dynamics.

As previously mentioned, China launched the BDS-3 satellite constellation in 2015 as part of a strategic initiative to join the Global Navigation Satellite System (GNSS). The inaugural phase of this initiative involved the launch of two experimental satellites into Medium Earth Orbit (MEO) on July 30, 2015. These satellites were designated as follows:

- Beidou-3S-M1S (originally identified by PRN C33)
- Beidou-3S-M2S (originally identified by PRN C34)

It is important to note that across the international community, various resources rely on the Pseudo-Random Noise (PRN) codes transmitted by navigation satellites to monitor and analyze the orbital environment. These PRN numbers serve as unique identifiers for individual satellites and are fundamental for tracking and understanding their movements in space. However, it is not uncommon for satellites to periodically exchange PRN numbers, especially when new satellites are launched, or existing ones are retired. Considering this practice, it becomes essential to meticulously track all PRN swaps, as these identifiers serve as a vital resource for monitoring and tracing each satellite's position.

This issue of PRN swaps arose during the process of identifying the interfering satellite. Following their launch in July 2015, the two BDS-3 experimental satellites underwent PRN number changes on the following two occasions:

- Beidou-3S-M1S: started transmitting by PRN C19 in November 2017 and started transmitting PRN C57 since September 2018
- Beidou-3S-M2S: started transmitting PRN C58 since 2018

However, it's important to note that several widely used almanac trackers incorrectly identify Beidou-3S-M1S as C58 even though it actually transmits PRN C57. This discrepancy can be readily verified by aligning a satellite dish with the sky and conducting a PRN code correlation analysis.

Fortunately, the U.S. Space Command (USSPACECOM) employs a unique method for identifying all celestial objects in space through the allocation of NORAD IDs. These NORAD IDs consist of sequential nine-digit numbers assigned by USSPACECOM, typically in the order of launch or discovery, to every artificial object situated within Earth's orbit, including those that have departed Earth's orbit. For example, the very first object cataloged, designated as NORAD ID: 1, corresponds to the Sputnik 1 launch vehicle, while the Sputnik 1 satellite is designated as NORAD ID: 2.

To avoid potential confusion associated with the PRN code identifiers, it is best to refer to the interfering satellite, Beidou 3S-M1S, using its NORAD ID: 40749.

## **5 IMPACT ANALYSIS**

After identifying the interfering satellite, the next objective was to assess its potential effects, if any, on receiver positioning. The impact analysis was focused on two separate concerns: 1) self-interference (the interference of N40749 on other Beidou signals), and 2) cross-interference (the effect of the N40749 on other GNSS constellations and signals).

### ***5.1 Self-Interference***

To understand how interference from 40749 might affect position data generated solely from Beidou signals, position accuracy was analyzed exclusively using Beidou satellites. The goal was to identify any noticeable variations in accuracy when satellite 40749 was within the line of sight when it was not. To conduct these tests, the following two receivers were used in distinct tracking signal configurations:

- TRIMBLE BX-992: Configured to track Beidou signals B1I and B3I for position data generation.
- Septentrio MOSIAC X5: Configured to track only the Beidou signal B3I for position data generation.

East-North-Up position data was collected at one-minute intervals to synchronize with the relative signal power entries. Upon continuous examination of the BX992 data for a 48-hour period spanning from August 10 to August 12, a significant rise in upward direction position error was evident when satellite 40749 entered the field of view. The dual-axis plot displayed below (Figure 17) shows the variations in position accuracy generated by the Trimble BX992. Its axes are defined as follows:

- X-axis: Time [UTC]
- Y-axis, left: Satellite Elevation [degrees]
- Y-axis, right: Positional Error [meters]

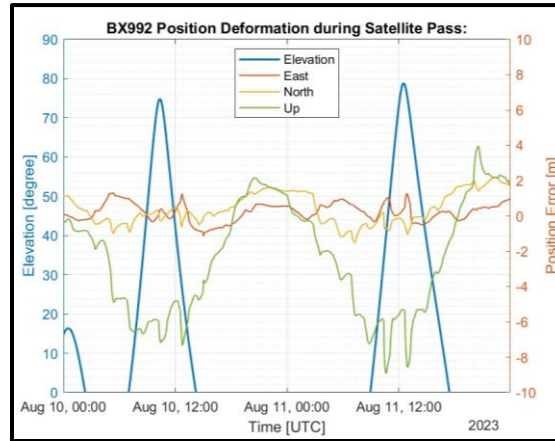


**FIGURE 17:** 48-hour monitoring of TRIMBLE BX992

However, after observing the position and FFT outputs continuously for a week, it became evident that the peaks in the up direction did not align perfectly with the interference peaks' time stamps nor the satellite ground track. For enhanced clarity, the plots below isolated position errors un the up direction to provide a more detailed understanding of error fluctuations during the satellite pass. The results are presented in Figure 18 below for the Trimble BX992, which tracked both B1I and B3I. The (3) axes on the plot are defined as follows:

- X-axis: Time [UTC]
- Y axis, right: Satellite Elevation [degrees]
- Y axis, leftmost: Positional Error [m]
- Y axis, second left: Relative Signal Power [dB]

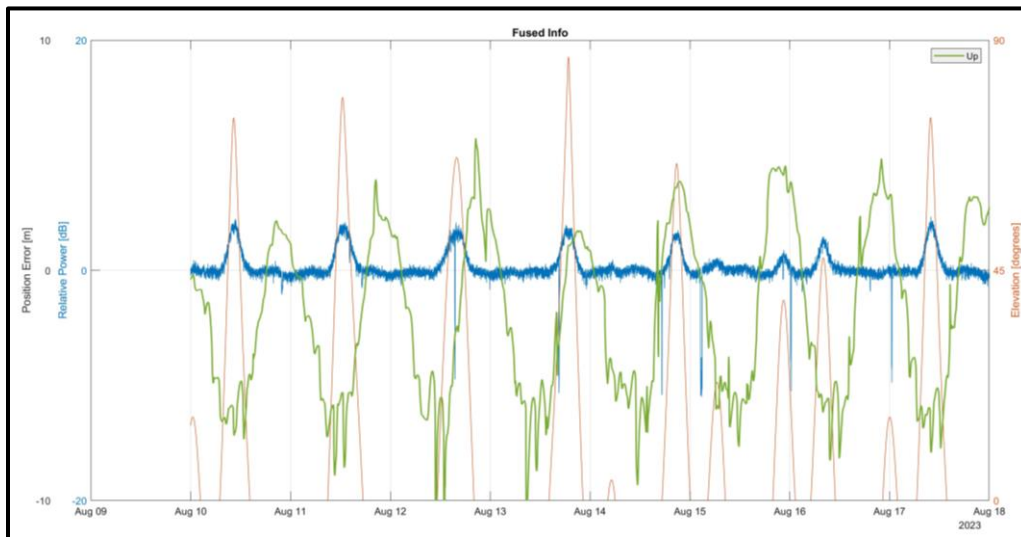


**FIGURE 18:** Position Tracking with TRIMBLE BX992 for one week

Figure 19 below shows a similar divergence of FFT vs position error oscillations for the Septentrio MOSAIC X5 receiver, which tracked only the B3I signal.

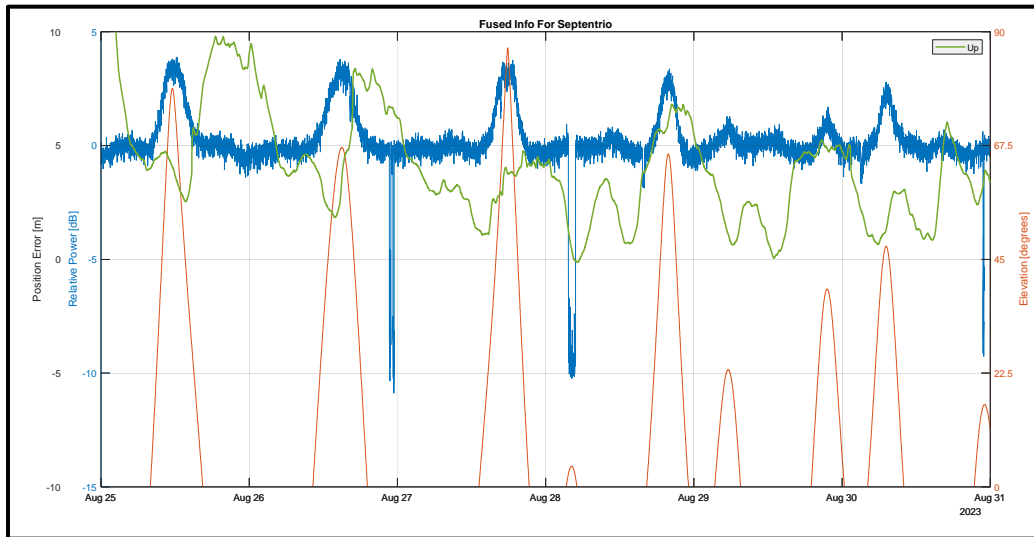


**FIGURE 19:** Position Tracking with Septentrio for one week

For both receivers, the peaks in the upward direction position error did not perfectly coincide with the ground track of Satellite 40749. However, those errors had a sinusoidal pattern that repeated approximately every 24 hours. This may be due to one of the corrections, e.g., the ionospheric correction due to its 24-hour periodicity.

To test this hypothesis, Trimble's Precise Point Positioning (PPP) corrected position solution was generated. The results confirmed no discernible presence of the sinusoidal variation in the up direction with the PPP solution. These results are shown in Figure 20 below:

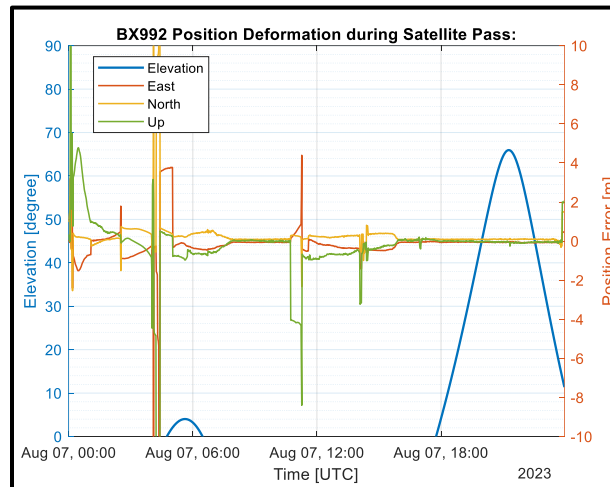


**FIGURE 19:** Positioning Solution with PPP Utilizing BX992

As evident from Figure 20, all positioning errors were notably absent when the satellite was within the receiver's line of sight. While there were some fluctuations present in the PPP solution, these fluctuations were attributed to localized events and changes in the PPP operating mode within the receiver itself. These were not linked to any impact from 40749. Consequently, it was determined that the interference originating from satellite 40749 did not create any measurable position inaccuracies. Self-interference effects from this interference on Beidou system appear to be minimal.

## 5.2 Cross-Interference

To evaluate the impact of cross-interference, it was first noted that the Beidou B3I signal has the most direct overlap with one main lobe of the Galileo PRS signal. (Figure 21 provides a visual comparison of this overlap between B3I and Galileo PRS.) This overlap indicates some potential 40749 to affect that signal in some way. However, since access to the Galileo PRS signal, data, and receivers are currently very strictly controlled, the authors were unable to perform further analysis for this paper.

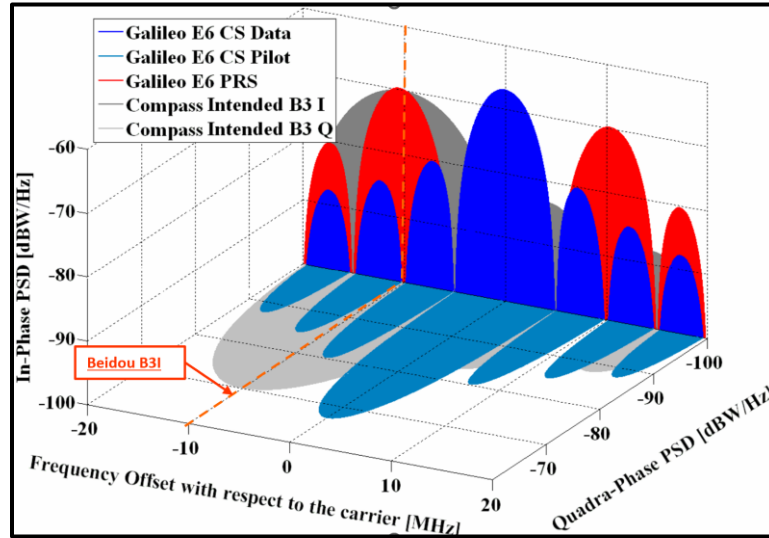


FIGURE21: B3I Overlap with Galileo PRS

## 6 CONCLUSIONS

In summary, our investigations, which involved analyses using Trimble's extensive Receiver Network and a 1.8-meter dish antenna, have yielded the following conclusions:

- 1. Positive Identification of Space-based Interference from a Satellite in MEO:**  
It has been conclusively determined that the observed interference indeed originates from a satellite situated in Medium Earth Orbit (MEO). This positive identification was critical for understanding the interferer's impact on satellite navigation systems.
- 2. Identification of Mislabeling between Beidou-3S-M1S [PRN57] and Beidou-3S-M2S [PRN58]:**  
A notable finding of this study is the verification of mislabeling between two Beidou satellites, specifically Beidou-3S-M1S (identified by PRN57) and Beidou-3S-M2S (identified by PRN58). This discrepancy in PRN labeling has been a potential source of confusion in satellite tracking and monitoring systems, and addressing this issue is essential for accurate satellite identification.
- 3. Addressing Previously Raised Questions:**
  - **Detection of Interference in B3I Waveform:** The presence of a narrowband interference spike in the B3I waveform has been observed, measured, and documented.
  - **Localization of Interference:** The study has successfully localized the source of the interference to satellite Beidou 3S-M1S, which can be unambiguously identified by its NORAD ID: 40749. This localization provides critical information for tracking and addressing the interference source.
  - **Characterization of Interference Impact:** Since the interference remains narrowly centered at 1268.52 MHz and has relatively low power, no discernible adverse impact on position accuracy on the Beidou system has been observed. This finding provides some assurance that, at the present state, the interference does not significantly affect any GNSS positioning performance. However, the Galileo PRS spectrum has some overlap with the frequency of interference. For completeness, this service should also be analyzed for any measurable effects from 40749.

## 7 ACKNOWLEDGEMENTS

The authors would like to thank Stuart Riley and Trimble Inc. for generously lending time, equipment, and other assistance with this investigation, and to the Aerospace Corporation for funding this research effort. The authors also would like to thank the FAA and Dr. T.S. Kelso, Operator of Celestrack.

## 8 REFERENCES

- Broumandan, A., Jafarnia-Jahromi, A., Daneshmand, S., & Lachapelle, G. (2016). Overview of Spatial Processing Approaches for GNSS Structural Interference Detection and Mitigation. *Proc. Of the IEEE*, vol. 104, no. 6, pp. 1246-1257.  
<https://doi.org/10.1109/JPROC.2016.2529600>
- Wang, P., Cetin, E., Dempster, Andrew G., Wang, Y. & Wu, S. (2018). GNSS Interference Detection Using Statistical Analysis in the Time-Frequency Domain. *Proc. Of the IEEE*, vol. 54, no. 1, pp. 416-428.  
<https://doi.org/10.1109/TAES.2017.2760658>
- Murrian, Matthew J., Narula, Lakshay, Humphreys, Todd E., (2019). Characterizing Terrestrial GNSS Interference from Low Earth Orbit," *Proceedings of the 32nd International Technical Meeting of the Satellite Division of The Institute of Navigation (ION GNSS+ 2019)*, Miami, Florida, September 2019, pp. 3239-3253.  
<https://doi.org/10.33012/2019.17065>
- Ferrara, N.G., Bhuiyan, M.Z.H., Söderholm, S. (2018). A new implementation of narrowband interference detection, characterization, and mitigation technique for a software defined multi-GNSS receiver. *GPS Solut* 22, 106  
<https://doi.org/10.1007/s10291-018-0769-z>
- Bhatti, J. A., Humphreys, T. E., and Ledvina, B. M. (2012). Development and demonstration of a TDOA-based GNSS interference signal localization system. *Proc. of the IEEE/ION Position, Location and Navigation Symposium*, Myrtle Beach, SC, USA, 2012, pp. 455-469.  
<https://doi.org/10.1109/PLANS.2012.6236915>
- Lindstrom, J., Akos, Dennis M., Isoz, O., & Junered, M., (2007). GNSS Interference Detection and Localization using a Network of Low-Cost Front-End Modules. *Proc. of the 20th International Technical Meeting of the Satellite Division of The Institute of Navigation (ION GNSS 2007)*, Fort Worth, TX, September 2007, pp. 1165-1172
- Thölert, S. & Antreich, F. & Enneking, C. & Meurer, M.. (2019). BeiDou 3 signal quality analysis and its impact on users. *Navigation*. 66.  
<https://doi.org/10.1002/navi.331>
- Yang, Y., Xu, Y., & Li, J. (2018). Progress and performance evaluation of BeiDou global navigation satellite system: Data analysis based on BDS-3 demonstration system. *Sci. China Earth Sci.* 61, 614–624  
<https://doi.org/10.1007/s11430-017-9186-9>